

# Narrow-spectral-span spectral beam combining with a nonparallel double-grating structure

Quan Zhou (周 权)<sup>1,2</sup>, Changhe Zhou (周常河)<sup>1,\*</sup>, Na Yu (于 娜)<sup>1,2</sup>,  
Chunlong Wei (韦春龙)<sup>1</sup>, Wei Jia (贾 伟)<sup>1</sup>, and Yancong Lu (卢炎聪)<sup>1,2</sup>

<sup>1</sup>Shanghai Institute of Optics and Fine Mechanics, Chinese Academy of Sciences, Shanghai 201800, China

<sup>2</sup>University of Chinese Academy of Sciences, Beijing 100049, China

\*Corresponding author: chazhou@mail.shcnc.ac.cn

Received April 11, 2017; accepted May 19, 2017; posted online August 2, 2017

We propose a nonparallel double-grating structure in a spectral-beam combining technique, where two gratings are placed nonparallel satisfying the Littrow mount in the focal region of the convergent lens. The most attractive advantage of this approach is that it will compress the spectral span into half of its original spectrum, which means the number of combined elements can be doubled in the gain range of diode lasers. Experimental results demonstrate that the CW output power of the combined beam is 30.9 W with a spectral span of 7.0 nm, compared with its original spectrum span of 13.6 nm, and the spectral beam combining efficiency is 70.5%. In consideration that a single grating could have a high efficiency of >97% in a bandwidth of over ten nanometers, the efficiency loss of the grating pair should be less than 6%, which is acceptable for most applications, so this method of using double gratings should be highly interesting for practical applications when a nearly doubled number of diode lasers could be combined into one single laser compared with the previous single-grating methods.

OCIS codes: 140.2010, 140.3290, 140.3298, 050.1950, 140.3410.

doi: 10.3788/COL201715.091403.

High-power diode lasers have been used in a variety of applications such as pumping of solid-state lasers and industrial manufacturing<sup>[1,2]</sup> (metal cutting, laser cladding, and laser marking) due to their advantages including a low cost, long lifespan, compact size, and so on. The output power of diode laser arrays have developed rapidly in recent years, for instance, a 1 cm 980 nm diode laser bar with a 1 kW quasi-CW output power has been obtained<sup>[3]</sup>. With the number of emitters increased, the output power of the diode laser array becomes higher naturally, however, the beam quality will get worse. One of the most promising approaches to achieving a high beam quality and high brightness beam is spectral beam combining (SBC). SBC technology has been verified to be a solution to combining beams from all the elements while maintaining the beam quality of a single element<sup>[4]</sup>.

Daneu *et al.* achieved SBC of an 11-element broad-stripe diode-laser array with a 1.8 W CW (continuous-wave) output power<sup>[5]</sup>. Chann *et al.* demonstrated a 35 W output power from a slab-coupled optical waveguide diode-laser array that contained 100 elements with a near diffraction-limited beam quality  $M^2 = 1.35$  by using SBC<sup>[6]</sup>. Gopinath *et al.* improved the structure of SBC by adding a telescope system to compensate the “smile phenomenon” and obtained a 20 W CW output power<sup>[7]</sup>. Zhang *et al.* achieved a 50.8 W CW output power with a 90.2% beam combining efficiency by using a transmission grating as the diffraction element<sup>[8]</sup>. Zhu *et al.* added a beam-shaping element called a “beam transform lens” to rotate beams 90°, and got a 58.8 W CW output power while the electro-optic conversion efficiency was 51%<sup>[9]</sup>.

For SBC methods, the number of combined emitters is not limited even if only one grating is theoretically used as the dispersion element. An obvious way to achieve a higher-power beam is by just combining more emitters<sup>[10]</sup>. Nevertheless, the number of emitters cannot increase infinitely because of the spectral span, since the whole spectral span of the SBC system will be broadened when the quantity of emitters increases, and the gain range of the diode laser is usually limited to tens of nanometers. In theory, if we suppose the diode laser gain range is 60 nm and the wavelength interval of adjacent emitters is 2 nm, 30 emitters can be combined in one SBC structure; but if the wavelength interval narrows to 1 nm, the quantity of combined emitters is doubled to 60, and the output power is also doubled at the same time. On the other hand, the maximum diffraction efficiency of a grating is at a specific wavelength, and the efficiency reduces while the wavelength deviates, therefore, the high-efficiency diffraction range of a grating is also confined. In consideration of manufacturing, fused-silica gratings can be obtained using holographic recording technology and inductively coupled plasma etching. In theory, the fused silica gratings can obtain a close-to-97% diffraction efficiency with a narrow bandwidth of over a 10 nm bandwidth, or greater than a 92% efficiency in a 100 nm bandwidth<sup>[11]</sup>. In addition, fused silica gratings have a high-power laser damage threshold, and SBC will benefit from the progress in gratings. In general, the spectral span greatly confines the number of emitters participating in SBC.

Improving the diffraction ability of the gratings can significantly narrow the whole spectral span of combined beams. For previous SBC structures, one grating was used

as the dispersion element with limited diffraction ability. In our experiment, two transmission gratings are applied in order to enhance the diffraction ability, and the spectral span narrowed down by 50% compared with the original SBC methods.

Compared with the previous parallel grating pair, in this experiment it is arranged particularly to narrow the spectral span by diffracting twice. The nonparallel gratings are both put in a Littrow mount, the divergence angle decreases by a half after the first grating and becomes parallel after the second grating, and the beams converge on the second grating at the same time.

In this Letter, two transmission gratings are employed in SBC of a 940 nm laser bar consisted of 19 emitters spaced at a 500  $\mu\text{m}$  pitch. The efficiency of the transmission gratings in the  $-1\text{st}$  order is over 94% with a period of 1500 lines/mm. The 30.9 W output power combined beam is obtained with a 7.0 nm spectral span, and the free running combining efficiency was 70.5%. The beam qualities  $M^2$  were 1.2 and 6.6 in the horizontal and vertical directions, respectively, at a low operating current.

Figure 1 is the schematic of SBC, and the basic structure resembles the previous structure, except there are two gratings. The basic elements include a diode-laser array, a fast axis collimator, a beam transformation system (BTS) lens, a slow axis collimator (SAC), a cylinder transform lens, two transmission gratings, and an output coupler.

To narrow down the spectral span, we use two transmission gratings instead of one grating as the diffraction

element. Each beam from the laser array has a unique incident angle on the gratings. The back facet of the laser array and the output coupler form a laser cavity, and beams get oscillated in this external cavity. After the beams are diffracted by the grating pair, only beams with a vertical incident angle on the output coupler can be reflected back to the laser emitters and get amplified. Therefore, all the beams are locked at monotonically typical wavelengths and have the same diffraction angle.

The diode-laser array used in this experiment is a common commercial 940 nm CW diode-laser array consisting of 19 emitters. The 19 emitters are placed horizontally and the width of each emitter is 500  $\mu\text{m}$ ; the active layer width is 100  $\mu\text{m}$  with a fill factor of 20%. The typical fast-axis divergence angle of a single element with 95% power is  $46^\circ$ , and the slow-axis divergence angle is  $9^\circ$ . In order to decrease the effect of the laser array's original resonators, the front facets of the laser emitters are antireflection coated.

The fast axis collimator (FAC) is a cylindrical lens that is placed to collimate laser beams in the fast axis. Beams are focused in the vertical direction so the divergence angles in the fast axis reduce to  $<0.5^\circ$ .

The BTS is a micro lens array used as beam-shaping element to rotate each single beam  $90^\circ$ . In another words, the fast axis was originally in the vertical direction and became in the horizontal direction after BTS, and contrarily, the slow axis changes oppositely. The beam-combining direction turns from the slow axis to the fast

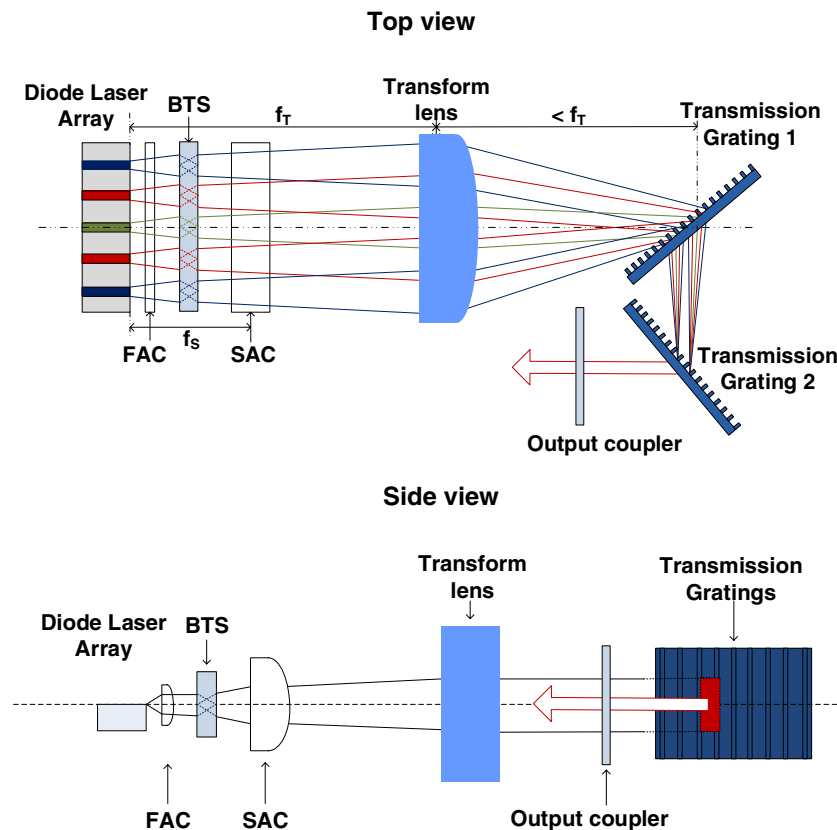


Fig. 1. Structure of beam combining.

axis. For an individual beam, the beam quality of the fast axis is much better than the slow axis, moreover, the slow axis is also affected by the smile phenomenon. Emitters are able to receive their own feedback more easily and accomplish beam combining when beams are combined on the fast axis.

The purpose of an SAC is similar to the FAC. After having the beams rotated, the slow axis is in the vertical direction, and the SAC is a cylindrical lens that aims to reduce the divergence angle on the slow axis. The focal length of the SAC is 60 mm.

The transform lens is placed between the laser array and the grating pair, and is one focal length away behind the laser array. The transform lens is also a cylindrical lens with a focal length of 300 mm, and it focuses all the beams on the gratings. The beam spots partially overlap on the first grating and completely overlap on the second grating.

The grating pair includes two transmission gratings (1500 lines/mm), and the efficiency of the  $-1$ st order is over 94%. The gratings should have a high diffraction efficiency for both TE- and TM-polarized waves because the diode-laser beams are polarized. Simplified modal methods are used to design  $-1$ st order high-diffraction efficiency gratings for polarization-independent waves, which are highly important for SBC<sup>[11-14]</sup>. Volume Bragg gratings could also be applied to SBC<sup>[15,16]</sup>.

The incidence angle of the central beam is a Littrow angle on both the first and the second grating to achieve the highest efficiency. The reflectivity of the output coupler is 10%. In traditional SBC structures, the grating is placed one focal length away from the transform lens to obtain a smallest beam spot on the grating. In double-grating structures, the first grating should be placed slightly less than one focal length away from the transform lens, and the second grating is a little behind the first grating to achieve the smallest beam spot on it.

The process of both traditional SBC and double-grating SBC will be shown as follows to explain how the spectral span can be narrowed to 50% in a double-grating structure.

Figure 2 is a simplified optical path of a traditional SBC, and the diffraction equation on the grating is

$$\Lambda(\sin \theta_i + \sin \theta_d) = m\lambda, \quad (1)$$

where  $\Lambda$  is the grating period,  $\theta_i$  is the incident angle, and  $\theta_d$  is the diffraction angle on the grating,  $m$  is the order, and  $\lambda$  is the wavelength. For the 1st order, the above equation can be expressed as a differential equation:

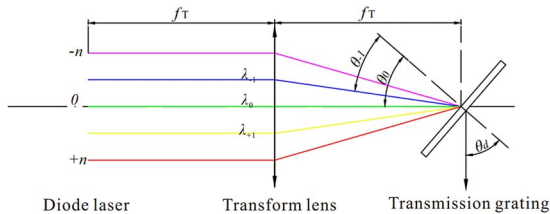


Fig. 2. Simplified optical path of a traditional SBC.

$$\Lambda \cos \theta_i d\theta_i = d\lambda. \quad (2)$$

The whole spectral span is<sup>[4]</sup>

$$\Delta\lambda = \frac{\Lambda \cos \theta_i \Delta x}{f}, \quad (3)$$

where  $\Delta\lambda$  is the wavelength span of the beams,  $\Delta x$  is the distance between the emitters on the array, and  $f$  is the focal length of the transform lens. As  $\lambda = 940$  nm,  $\Lambda = 1/1500$  mm and  $f = 300$  mm, it can be considered that  $\theta_i = \theta_d = \theta_{\text{littrow}} = 44.8^\circ$ . The calculated whole spectral span is 14.2 nm.

Figure 3 is the optical path of the double-grating SBC. The theoretical derivation of the double-grating SBC is similar to the above. The differential equation on the first grating is

$$\Lambda \cos \theta_i d\theta_i + \Lambda \cos \theta_d d\theta_d = d\lambda. \quad (4)$$

As all the beams have the same diffraction angle after the second grating, the differential equation is simplified as follows:

$$\Lambda \cos \theta_{i2} d\theta_{i2} = d\lambda. \quad (5)$$

The incident angles on the two gratings are both Littrow angles so that  $\theta_i = \theta_d = \theta_{i2} = \theta_{\text{littrow}} = 44.8^\circ$ , and  $d\theta_d = -d\theta_{i2}$ . The spectral span is

$$\Delta\lambda = \frac{\Lambda \cos \theta_i \Delta x}{2f}. \quad (6)$$

The calculated spectral span is 7.1 nm. Comparing Eqs. (3) and (6), it can be concluded that the spectral span of a double-grating structure SBC is only half of the spectral span of traditional SBC methods under the condition that other parameters, including the position and the number of emitters, remain unchanged. Double elements could be combined in the limited gain range of diode lasers.

Additionally, the spectral span is inversely proportional to the focal length of the transform lens in Eq. (6), therefore, if we abnegate the advantage of narrowing the spectral span and keep the spectral span the same, the focal length of the transform lens could be reduced by half, which means the SBC system would have a smaller size and a lighter weight.

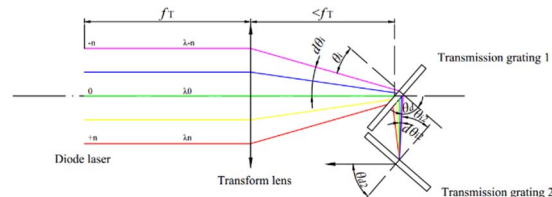


Fig. 3. Simplified optical path of the double-grating SBC.

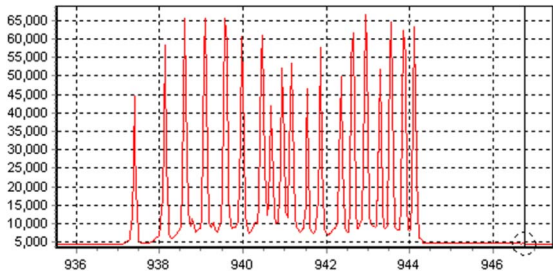


Fig. 4. Spectrum of the double-grating SBC laser.

Figure 4 is the spectrum of the double-grating SBC laser. There are 19 peaks in this image, representing 19 beams from the emitters. The whole spectral spread is about 7.0 nm, which agrees with the calculated value. On account of the smile phenomenon, the distortion of the emitters caused by thermal effect, the emitters deviate in the vertical direction. This deviation is rotated by the BTS and becomes a horizontal disparity, which induces the inequalities of the wavelength interval between neighboring emitters. Figure 5 shows the spectrum of a traditional SBC structure. The spectral span in Fig. 5 is 13.6 nm, so this spectral compression method is proved in the experiment.

In addition, the central wavelengths in Figs. 4 and 5 are slightly different. The reason is that the incident angles on the gratings are subtly changed in the two experiments, so the central wavelengths are locked at different values.

The double-grating SBC and free running output powers are both shown in Fig. 6. Furthermore, the electro-optical conversion efficiency and driving voltage are also included. The maximum power of the double-grating SBC is 30.9 W with an electro-optical conversion efficiency of 27.1% at 60 A. The free running power at 60 A is 43.8 W, so the beam combining efficiency is 70.5%, which is the ratio of the SBC power to the free running power.

The main loss during the combining process is the reflectivity from all these elements. Any reflectivity may form a subcavity and decreases the combining efficiency; if the optical components were antireflection-coated the efficiency will be higher. On the other hand, on the condition that the loss in the laser cavity is reduced, the reflectivity of the output coupler can also be lowered, and the optical efficiency can also be better.

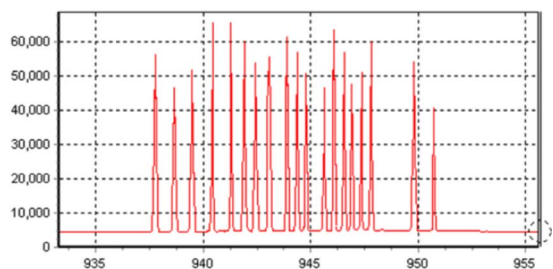


Fig. 5. Spectrum of the single-grating SBC laser.

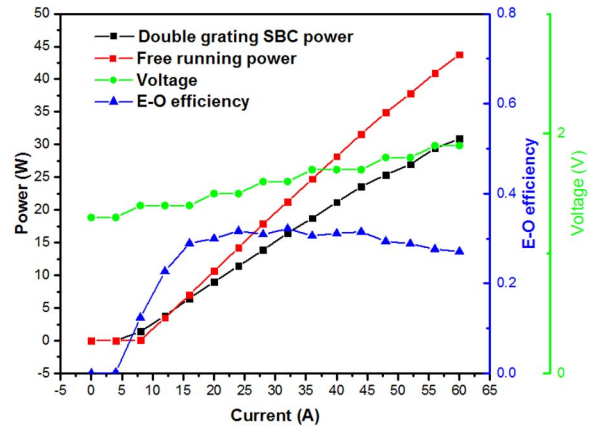


Fig. 6. Output power and efficiency of the double-grating SBC laser, 30.9 W output power, and 70.5% efficiency is demonstrated.

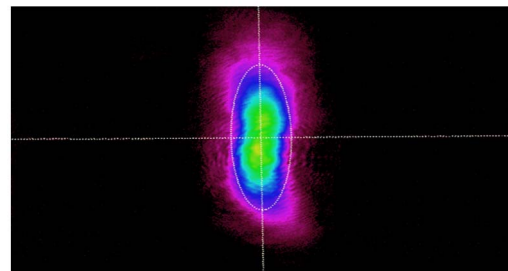
As it is antireflectivity coated on front facet of the laser array, the free running threshold current increases to 9 A, and is larger than the SBC threshold current of 5 A. When the operating current is near the threshold current, the SBC power may be higher than the free running power.

Figure 7 shows the beam quality and the beam spot after SBC. The output beam is focused by a 50 mm focal length lens and measures by a beam quality analyzer. The beam quality  $M^2$  is 1.2 on the fast axis at a 20 A operating current. In contrast, the beam quality on the slow axis is 6.6 at 20 A.

In conclusion, a new method of SBC with a double-grating structure is demonstrated in this Letter, and the spectral span is only a half of that compared with traditional methods; identically, the experimental setup size could be decreased to nearly a half if the spectral span is maintained. We achieve 7.0 nm spectral span output

M <sup>2</sup> Results		
	X	Y
M <sup>2</sup>	1.1998	6.6018
Divergence (mrad)	6.744	5.898
Waist Width (mm)	0.213	1.340
Waist Location (mm)	191.96	217.07
Rayleigh Range (mm)	31.57	227.12

(a)



(b)

Fig. 7. (a) Beam quality after SBC. (b) The output beam spot.

beams by using two transmission gratings as diffractive elements to improve the diffractive ability. The output power of SBC is 30.9 W with a free running combining efficiency of 70.5%, and the electro-optical conversion efficiency is 27.1%. Furthermore, the combining efficiency of the double-grating SBC can be increased remarkably by reducing the loss in the external cavity. Meanwhile, the reflectivity of the output coupler can also be optimized.

With the spectral span narrowed down, we can add more emitters in SBC to take full advantage of the gain range of the diode-laser material and the high diffraction range of the gratings. It provides us a promising method to develop a diode laser with a higher output power and brightness.

This work was supported by the Shanghai Science and Technology Committee (Nos. 16DZ2290102 and 15JC1403500), the Chinese Academy of Sciences (No. QYZDJ-SSW-JSC014), and the National Natural Science Foundation of China (No. 61405216).

### References

1. F. Bachmann, *Appl. Surf. Sci.* **208**, 125 (2003).
2. X. Yang, Y. Yin, X. Li, S. Xu, Y. Xia, and J. Yin, *Chin. Opt. Lett.* **14**, 071403 (2016).
3. D. Schröder and D. Lorenzen, *Proc. SPIE* **6456**, 64560N (2007).
4. C. C. Cook and T. Y. Fan, *Adv. Solid-State Lasers* **26**, 163 (1999).
5. V. Daneu, A. Sanchez, T. Y. Fan, H. K. Choi, G. W. Turner, and C. C. Cook, *Opt. Lett.* **25**, 405 (2000).
6. B. Chann, R. K. Huang, L. J. Missaggia, C. T. Harris, Z. L. Liau, A. K. Goyal, J. P. Donnelly, T. Y. Fan, A. Sanchez-Rubio, and G. W. Turner, *Opt. Lett.* **30**, 2104 (2005).
7. J. T. Gopinath, B. Chann, T. Y. Fan, and A. Sanchez-Rubio, *Opt. Express* **16**, 9405 (2008).
8. J. Zhang, H. Peng, X. Fu, Y. Liu, L. Qin, G. Miao, and L. Wang, *Opt. Express* **21**, 3627 (2013).
9. Z. Zhu, L. Gou, M. Jiang, Y. Hui, H. Lei, and Q. Li, *Opt. Express* **22**, 17804 (2014).
10. C. E. Hamilton, S. C. Tidwell, D. Meekhof, J. Seamans, N. Gitkind, and D. D. Lowenthal, *Proc. SPIE* **5336**, (2004).
11. H. Cao, C. Zhou, J. Feng, P. Lv, and J. Ma, *Appl. Opt.* **49**, 4108 (2010).
12. S. Wang, C. Zhou, Y. Zhang, and H. Ru, *Appl. Opt.* **45**, 2567 (2006).
13. W. Sun, P. Lv, C. Zhou, J. Wu, and S. Wang, *Chin. Opt. Lett.* **11**, 070502 (2013).
14. J. Wu, C. Zhou, H. Cao, A. Hu, W. Sun, and W. Jia, *Chin. Opt. Lett.* **11**, 060501 (2013).
15. J. Feng, X. Zhang, D. Wu, S. Wu, and X. Yuan, *Chin. Opt. Lett.* **13**, S10901 (2015).
16. X. Zhang, F. Gao, J. Feng, K. Zou, B. Xiong, and X. Yuan, *Chin. Opt. Lett.* **12**, 030901 (2014).